

SQUARE-WAVE OPERATION OF A THERMAL CONDUCTIVITY DETECTOR

by

SUNTAY HAYRI EDIZ

B. S., Wabash College, 1967

9984

A MASTER'S THESIS

submitted in partial fulfillment of the

requirement for the degree

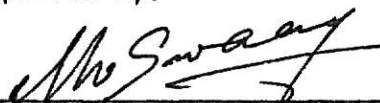
MASTER OF SCIENCE

Department of Chemistry

KANSAS STATE UNIVERSITY
Manhattan, Kansas

1970

Approved by:



Major professor

LD
2668
T4
1970
E3
copy 2

To My Parents

ILLEGIBLE

**THE FOLLOWING
DOCUMENT (S) IS
ILLEGIBLE DUE
TO THE
PRINTING ON
THE ORIGINAL
BEING CUT OFF**

ILLEGIBLE

**THIS BOOK
CONTAINS
NUMEROUS PAGES
WITH DIAGRAMS
THAT ARE CROOKED
COMPARED TO THE
REST OF THE
INFORMATION ON
THE PAGE.**

**THIS IS AS
RECEIVED FROM
CUSTOMER.**

TABLE OF CONTENTS:

List of Figures	iii
Introduction	1
Literature Survey	8
Construction	15
Symbols	17
Electronic Circuits	18
Regulated Power Supply	19
Smoothed High Current Supply	22
Oscillator and Clamps	24
Current Boosters and Common Mode Rejection Amplifier	29
Preamplifier, Demodulator and Attenuator	32
DC-AC Switching System	35
Complete Circuit	37
Bridge Control System	40
Front Panel	42
Parts List and Socket Pin Connections	
Regulated Power Supply	44
Smoothed High Current Supply	47
Oscillator and Clamps	51
Current Boosters and Common Mode Rejection Amplifier	54
Preamplifier and Demodulator	58
DC-AC Switching System	61
Parts List	
Bridge Control System	64
Attenuator	64

Operation	65
Data and Discussion	66
References.	69
Acknowledgement	72
Vita	73
Abstract	

LIST OF FIGURES:

Figure 1	Graph of response of a detector vs. sample concentration. Relation between sensitivity and detection limit is shown.	5
Figure 2	a. Schematic diagram of thermal conductivity detector powered by dc current. b. Schematic diagram of thermal conductivity detector powered by square-wave ac current.	6 6
Figure 3	Possible ac wave forms that may be used to power thermal conductivity detector. Relation between voltage and power is indicated. a. Sinusoidal ac b. square-wave ac lacking vertical symmetry c. square-wave ac lacking horizontal symmetry d. symmetrical square-wave ac	7
Figure 4	Katharometer cell designs. a. Flow-through b. Convection-Diffusion c. Self-purging	10
Figure 5	Circuit diagram for regulated power supply.	20
Figure 6	Circuit diagram for smoothed high current supply.	23
Figure 7	Circuit diagram for oscillator and clamps.	26
Figure 8	Simplified schematic of clamping circuit.	27
Figure 9	Circuit diagram for current boosters and common mode rejection amplifier.	31
Figure 10	Circuit diagram for preamplifier, demodulator and attenuator.	34
Figure 11	Circuit diagram for dc-ac switching system.	36
Figure 12	Complete circuit; oscillator and clamps, common mode rejection amplifier and current boosters, dc-ac switching system, preamplifier and demodulator.	39
Figure 13	Circuit diagram for bridge control system.	41
Figure 14	Front panel of the instrument.	43
Figure 15	Etch pattern board I, foil side.	46
Figure 16	Etch pattern board II, foil side.	50
Figure 17	Etch pattern board III, foil side.	53

Figure 18	Etch pattern board IV, foil side.	57
Figure 19	Etch pattern board V, foil side.	60
Figure 20	Etch pattern board VI, foil side.	63
Figure 21	Results.	68
	a. Peak obtained with .2 μ l air sample when bridge was powered with ac current.	
	b. Peak obtained with 10 μ l air sample when bridge was powered with dc current.	
	c. Peak obtained with 10 μ l air sample when bridge was powered with ac current.	

INTRODUCTION:

The measurement of thermal conductivity of gases goes back as far as 1840, but major studies have started early in the 20th century. In 1912, Langmuir¹ studied convection and conduction of heat in gases. Later in 1921, Shakespear² constructed an instrument to determine the purity of gas streams. He called his apparatus a "katharometer." In 1933, Daynes³ published a book on gas analysis by thermal conductivity. In 1946, Claesson⁴ measured the composition of binary and complex gaseous mixtures. Ever since, this method of analysis of gases has been employed as a major detection system in conjunction with gas chromatography.

Presently used thermal conductivity cells consist of four heat-sensing elements incorporated into a Wheatstone bridge circuit⁵, and positioned in a block made of aluminum, brass or stainless steel, heaters for the block, and a thermocouple to measure the temperature of this block. The heat sensing elements, which may be thermistors or resistance wires, are chosen so that their electrical resistance varies with temperature. They are placed in the separate cavities of the block, and heated by a constant current. Carrier gas must flow through these cavities whenever power is supplied, to prevent overheating of the filaments.

The temperature of the filaments reaches a certain constant temperature when the heat loss from the filaments to the carrier gas equals the heat supplied to the filaments from the power supply. Under these circumstances, the bridge output is adjusted to zero by means of one or more trimming circuits.

The heated filaments lose heat through radiation, conduction to the block through the thermal connections, forced convection and thermal

conduction to the gas stream. The latter two processes are usually dominant. If a carrier gas such as hydrogen or helium is used, then heat conduction due to gaseous conduction dominates. Heat loss is a complex phenomenon, and it is a function of bridge current, bridge resistance, thermal conductivity of sample gas and carrier gas, cell geometry, type and number of filaments.

The thermal conductivity detector is a concentration sensitive detector. It responds to those gases that have different thermal conductivities than that of the carrier gas. It would not differentiate between different species with nearly identical thermal conductivities, but it would produce an additive signal. Better sensitivity and better linearity are produced if a carrier gas of high thermal conductivity is used⁶. Of the two most highly conducting gases, hydrogen and helium, helium is used because it does not constitute an explosion hazard.

Since the stability of the detector depends strongly on detector temperature control, the detector block must be controlled within at least 0.05°C . The temperature throughout the detector block must also be uniform. Temperature changes at the filaments may be as small as 10^{-4}°C ⁵.

Linearity of response over a wide dynamic range of sample concentration, Fig. 1, is one of the most important factors in the performance and evaluation of a thermal conductivity detector. Linearity of a detector largely depends on operating conditions. Sometimes, the manipulation of the detector parameters to draw linear graphs may tend to de-emphasize gross linearity errors⁷. The linear dynamic range of a thermal conductivity detector is 10^4 -fold (up to about 1%)⁵.

The detection limit, which is approximately 1 ppm for a conventional

thermal conductivity detector⁵, is defined as the sample concentration producing a signal equal to twice the noise level. Sensitivity and detection limit are related but they are not synonymous. The achievement of higher sensitivity does not necessarily mean a decrease in detection limit, since detection limit may be defined as $2(\text{noise level/sensitivity})^8$, Fig. 1.

When the sample gas elutes from the chromatographic column, it passes through the sensing elements of the detector, and less heat is transferred from the sensing elements. If the temperature of the block and the flow rate of the carrier gas are held constant, a change in temperature of the filament occurs, producing an unbalance in the associated Wheatstone bridge. This unbalance is recorded as a signal. As soon as the sample gas is removed from the hot sensing elements, the bridge returns to its original condition.

The Wheatstone bridge of the thermal conductivity detector is conventionally powered with a dc current. The output is then also a dc current which may serve as an input signal to a potentiometric recorder. Most recorders include an input chopper and ac amplification. With a conventional 1 mV recorder, it appears that the detection limit is controlled by the recorder, and not by the bridge⁹, Fig. 2a. Therefore it is apparent that a better read-out system is needed.

If a chopper is placed before the bridge, rather than at the output terminals, the bridge unbalance signal would be an ac signal of known phase and frequency, which could easily be amplified, after which noise signals could be rejected by means of synchronous rectification¹⁰. A major advantage of this approach is the elimination of critical low level choppers, and rejection of all thermal EMF's in the bridge circuit.

Accordingly, we decided to design and construct an ac bridge supply and output preamplifier to determine the detection limits attainable with such an instrument.

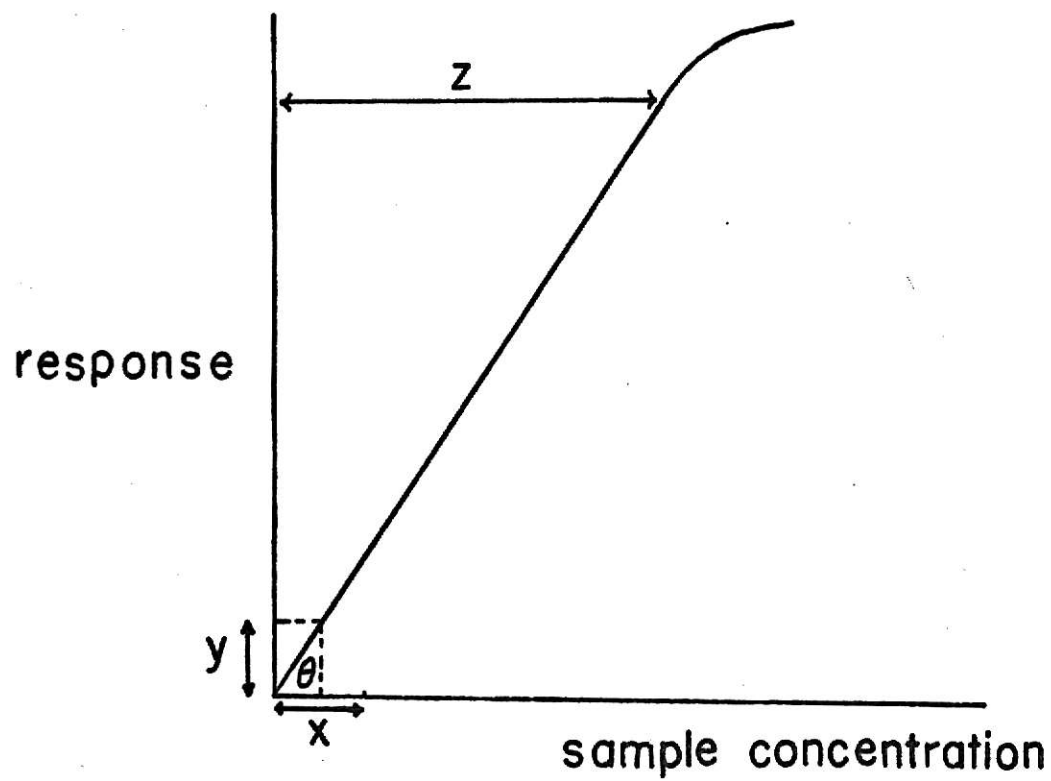
If varying current is applied to the elements of the bridge, problems such as thermal vibrations, and periodic magnetic interactions between the loops of the filaments may arise. This may not only damage the filaments, but it may also give rise to thermal noise.

If the voltage supplied to the bridge is sinusoidal ac, power will vary as a function of time, since power is directly proportional to the square of the current. The filaments will heat up during the first $1/4$ cycle and cool down during the next $1/4$ cycle, Fig. 3a.

To eliminate the problems mentioned above, a perfectly symmetrical square-wave ac should be applied. This will result in constant power at the filaments at all times, Fig. 3d. The vertically dotted lines indicate the transients during the $1/2$ cycles. Their effect may be made small enough to make any variations in power negligible.

If the square-wave ac lacks vertical symmetry, the power delivered to the filaments will have two distinct values during each cycle of the square-wave ac, Fig. 3b. Therefore, the vertical symmetry in the applied square-wave ac is crucial. If the square-wave ac lacks horizontal symmetry, the power at the filaments of the bridge will still be constant, Fig. 3c.

The upper two rows in Fig. 3 illustrate the considerations of the type of ac voltages applied at the inputs of the bridge. A and B have equal magnitude but they are out of phase by 180° .



z. dynamic range

y. noise

x. detection limit = $2y \cdot \cot \theta$

$\tan \theta$. sensitivity

Fig.1

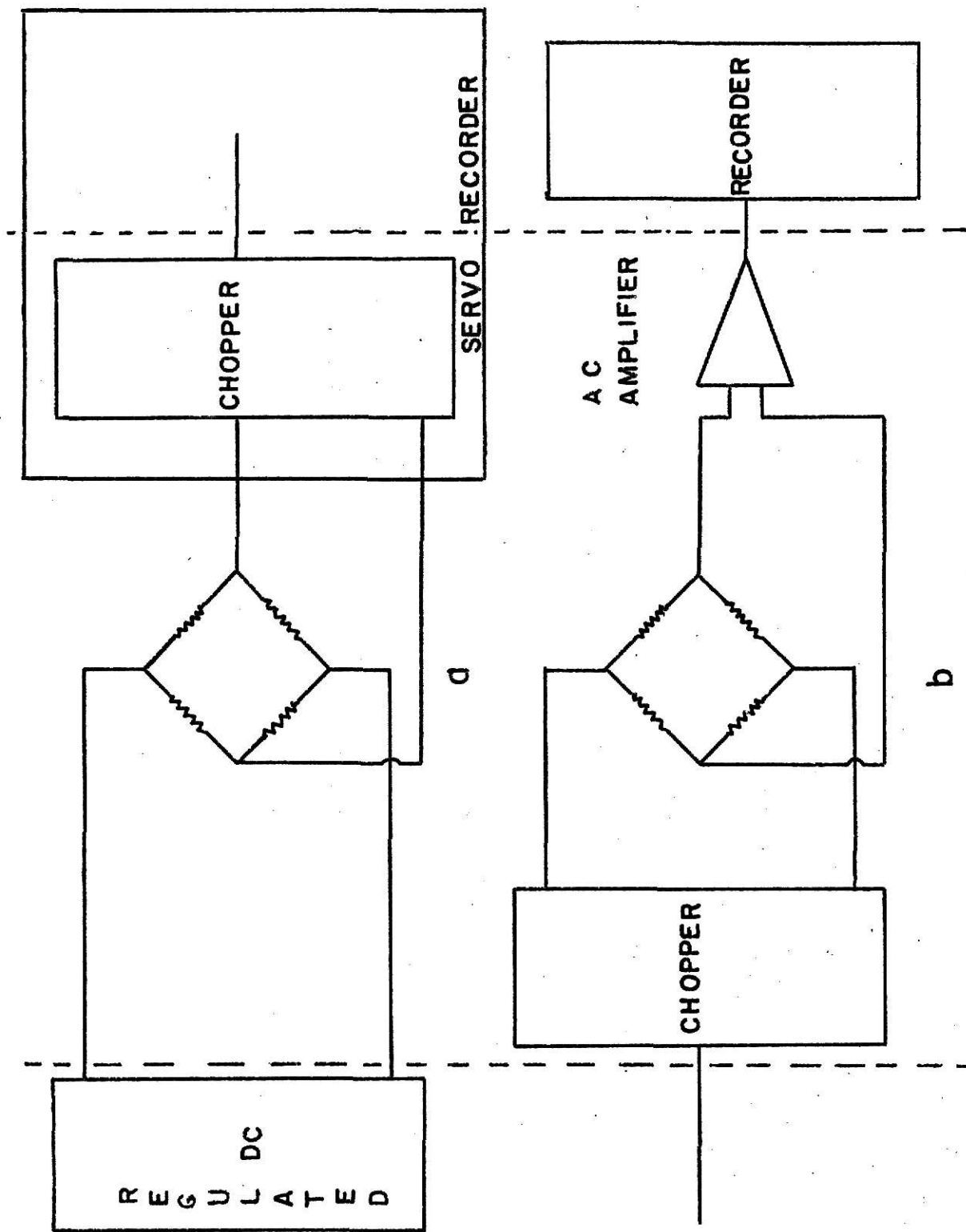


Fig.2

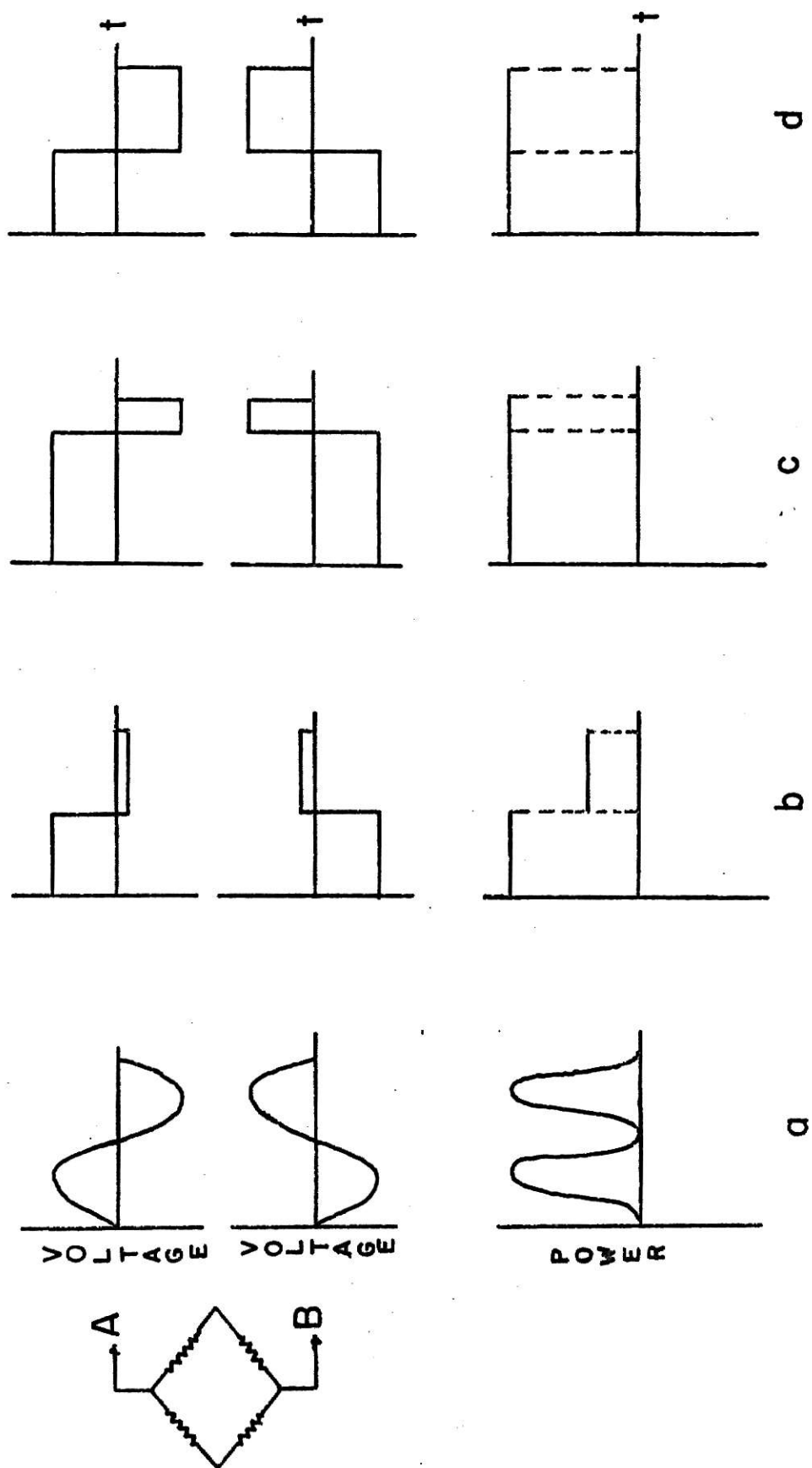


Fig.3

LITERATURE SURVEY:

A number of investigators have studied the problems associated with enhancing the sensitivity and increasing the detection limit of the katharometer. They have attempted to achieve this through mechanical and electrical means.

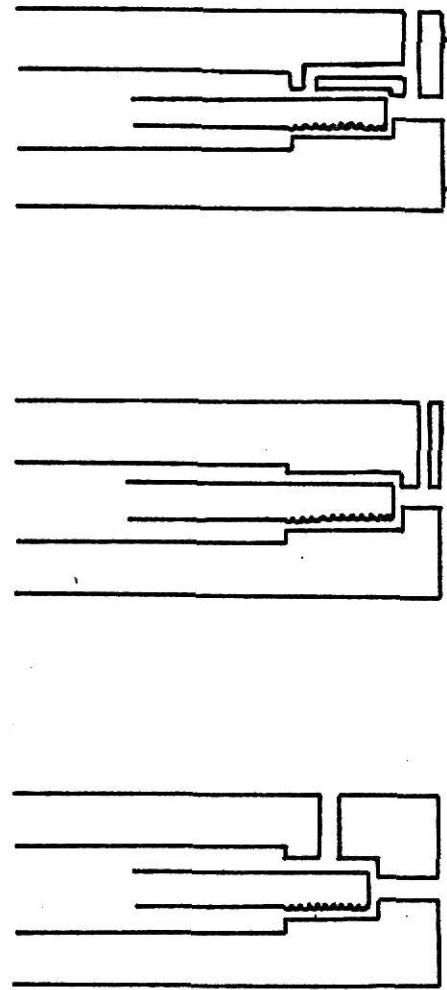
Extensive work has been reported by Keulemans¹¹, who verified that the katharometer sensitivity was largely determined by the amount of current supplied to the sensing elements¹², cell geometry¹³, thermal conductivity of the carrier gas¹⁴, and the temperature of the detector block¹⁵. Current increase, which causes a higher temperature difference between the sensing element and the detector wall, strongly influences the sensitivity, but baseline stability becomes a limiting factor as to the amount of current that can be employed^{11, 16, 17}. Hoffmann¹⁸ increased the temperature gradient by cooling the block, rather than increasing the filament temperature. Increase in current has another drawback: catalytic reactions may occur at the filaments at higher temperatures when H₂ is used as a carrier gas. This results in fouling of the sensing elements, whose sensitivity is thereby masked to a great extent^{11, 12}. This problem can be eliminated by coating the sensing elements with glass. Under these circumstances, good sensitivity, low drift, reasonably fast response, and high mechanical stability of the sensing elements have been reported^{19, 20}. Obermiller et.al.²¹ have clad the tungsten filaments with Teflon, and proved that they were far superior to the bare tungsten filaments. A non-corrosive thermal conductivity cell made out of glass or quartz has also been reported, with its sensing elements surrounded by a tightly packed aluminum powder²².

It has been shown that a direct relationship exists between the design of the cell or cell geometry, the location of the filaments in the cell with respect to the gas stream, and the flow sensitivity of the time constant or response time of the detector^{8,23}. Of the three types of cell designs which are illustrated in Fig. 4, the self purging produces the best time constant, which is directly proportional to the volume, and a low flow sensitivity. With the modified design of diffusion-type four-filament cell, the signal is independent of flow rate fluctuations at flow rates higher than a certain minimum value²⁴.

Soma et al.²⁵ have achieved lower detection limits with thermistor sensors. They enclosed one of the sensing elements in a cavity covered with a membrane permeable to gases, while the other one was contained in a cavity covered with an impermeable membrane. These authors obtained rapid response time and noted a decrease in detection limit due to self-heating effect of the thermistors with currents of about 2 mA. Temperature differences were measured with a differential amplifier; the noise level was less than 0.1 μ V.

Sensitivity of the filaments has been found to be roughly proportional to the product of the resistivity, ρ , and the square root of the temperature, T , of the wire. Platinum and tungsten are the most popular metals used for the sensing elements. Bismuth and antimony have the highest product of the two properties mentioned above, but unfortunately these metals cannot be drawn into wire¹¹.

The use of V-shaped filaments to achieve higher sensitivity has been reported in the literature²⁶, but the most common design has been the helical type which permits the insertion of long wires into the small bores of the detector block¹¹. Different sensitivity values have been reported



a. flow-through b. convection-diffusion c. self-purging

KATHAROMETER CELL DESIGNS

Fig. 4

for filaments coiled into single and double helices²⁷.

Efforts have been made to minimize the dependence of the sensitivity on the flow of the gas stream. Two fine metal screens have been wrapped around the thermistor bead. The inner screen decreased the effect of the gas flow at least 10-20 fold, while the second screen eliminated the effects arising from mechanical vibrations. The transient output of the detector at the time of sample introduction was 20 μV compared to 2 mV for the unscreened thermistor. When another screen was added, the response to the pressure transient on injection was 1 μV ^{28,29,30}. Modell³¹ placed the sensing element, a thermistor or a hot wire, in the center of a cylindrical screen bed packed with hollow glass spheres, particle size of about 30-125 μ . The sensing element then was placed perpendicular to the gas stream. The reference element was supplied with gas from an independent source. The author reported that sensing elements became relatively insensitive to flow above gas velocities of 30 cm/sec. The response time of the packed-bed sensing elements was 1.5 times that of the screened thermistor at high flow rates. The noise level in laminar flow was not measured. In turbulent flow, the packed-bed is superior; noise level was about 0.2 mV because turbulence cannot penetrate the packed-bed, and only heat loss from the screen varies. This variation becomes unimportant as thermal resistance from the screen decreases with increasing flow rate.

Better detection limits are also attainable through proper modifications of the power supply to the thermal conductivity cell, mechanical variation of the Wheatstone bridge, and handling of the output signal. Hannah³² replaced the zinc-carbon 9-volt dry cell battery with an 8.4-volt nickel-cadmium battery. The latter is advantageous in that it supplies

steady power and it is rechargeable. Littlewood³³ connected a resistor in parallel with the sensing elements and another resistor in series with them to reduce baseline drift. He also eliminated the problem arising from temperature and voltage controls, and consequently achieved a better detection limit.

Above the self-heating point, thermistors have a negative incremental resistance. This may give rise to a negative output impedance of a Wheatstone bridge, with potentially very high gain under loaded conditions. Attendant time constants make this impractical³⁴. The Du Pont-ERL bridge^{30,33} was developed to null out power supply noise by matching noise sensitivities. This is done by unbalancing the currents in the two legs in such a way that the response of two thermistors to power supply noise are equal. The same approach can be used for temperature variations. The advantage of the Du Pont-ERL bridge is in that it nulls out either the noise arising from the current or the temperature. Buhl³⁴ uses the Du Pont-ERL technique to attain a temperature null and adds resistors in parallel with the sensing elements to achieve current nulling. With this, the bridge would always have a non-zero output which can be remedied by a dc offset system, although with sub microvolt output signals, stability may be hard to achieve.

Madden et al.³⁵ observed that a thermal conductivity bridge powered by ac produced a poor resistive balance. With 50-cycle ac power, they obtained a good residual balance potential. By placing a Twin-T filter tuned to 150 Hz in the amplifier circuit, they removed the 2nd harmonic signal and thereby improved the null point of the thermal conductivity bridge.

Attempts have been made by a few investigators to amplify the dc output

of the thermal conductivity bridge^{36,37}. Burg et al.³⁷ placed a manganin resistor across the amplifier to reduce the input impedance. Bennet et al.³⁶ did not have a feedback circuit on their amplifier, so that amplification varied as the attenuation of the bridge changed. They reported the effective full scale to be between 40-1000 μV , but chose a 25 μV range for the experimental work. The noise level at the bridge was given as 0.1-0.2 μV . A drift of about 5.0-10.0 μV was noted. Fluctuations at the thermistors were the primary reason for the drift. The amplifier was linear at signals less than 300 μV .

In view of the complications and sensitive instrumentation required when dc operated thermal conductivity detectors are used, Furst et al.³⁸ employed an ac current produced by a 1000 Hz vacuum tube oscillator to operate the katharometer. The current was amplified by a second tube and coupled to the bridge by a center-tapped transformer to give a push-pull drive. The authors indicate a variation of sensitivity through gain control and also the possibility for logarithmic response through use of remote cut-off tubes, indicating that their amplifier was probably open-loop, so that they must count on gain stability. The bridge output was rectified without phase discrimination, i.e. bridge unbalance in both directions would give a positive dc output. There is no claim for increased sensitivity.

Kieselbach³⁰ studied the various sources of noise in thermistor detectors and verified that the principal contributors were external to the thermistor. These are bridge-current, flow, ambient temperature variations, shock and vibration. The author eliminated leakage to ground in the wiring by bringing the common mode of the detector bridge output to ground

potential; mismatch of the resistances of the thermistors was decreased by operation at the same temperature rather than at the same current. Kieselbach improved stability at the expense of a small loss in sensitivity by having higher resistance loads which minimized the effects of stray resistance and thermal emfs in cables and connectors between the detector and the remainder of the bridge circuit. The noise arising from the servo amplifier was negligible when compared to that of the main noise. Through his modifications, he achieved a 50-fold improvement in the S/N (signal to noise) ratio over the conventional design.

Papers by Grice and Winefordner, though not related to thermal conductivity detectors should be mentioned here. Grice et al.³⁹ describe an ultrasonic cell which is capable of detecting 0.5 ppm H₂ in argon. This is comparable to the performance of our system. The cell in its present form is limited to temperatures of 200°C; furthermore, the system is not compatible with the thermal conductivity blocks which are a part of the vast majority of gas chromatographs in use today. Winefordner et al.⁴⁰ describe detectors which are based on the dielectric properties of gas mixtures which may be monitored either by frequency of an RF oscillator, or by the RF field distribution in a capacitor containing the sample gas. Detection limits vary from 2-8 ppm for most gases. The dynamic range was reported as 10² to 10⁴.

CONSTRUCTION:


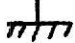



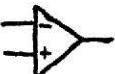
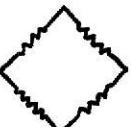
Nearly all of the components of our solid-state instrument are mounted on 4" x 4" copper-plated circuit boards. First the circuit lay-out is drawn on a 4" x 4" paper which is pasted to the board. Holes corresponding to the location of the component leads are drilled with 3/64-inch drill bit. The portion of the board that fits into the socket is inserted into the socket so that metal contacts in the female part make traces on the copper to assure proper location of edge contacts. The boards are cleaned with acetone, marked with a resist marking pen (RMP-700), and etched in a warm solution (20%, w/w) of ammonium persulfate. Then the boards are rinsed with water and acetone respectively to reveal the design. The components are soldered. The foil side of the boards except the edge contacts are sprayed with "clear acrylic spray" to prevent air oxidation of copper. The circuit boards are inserted into 15-pin socket connectors which in turn are fastened to an aluminum chassis, to provide connections between different socket pins.

Commercial and home-made heat dissipators are used on transistors where large amounts of heat are produced. The size of a heat dissipator depends upon ambient temperature and the maximum average power that the transistor dissipates. Transistors on the same board having a common collector connection may be inserted into a single aluminum heat dissipator. Those transistors which do not have a common collector connection obviously must have separate heat sinks.

In circuits where low level signals are handled, special attention must be given to system grounding. There is always a certain amount of potential drop between multiple grounds in a single circuit resulting from inductive

and/or capacitive coupling between the presumably isolated circuits. This may result in sufficient cross-talk to mask the millivolt or low level signal. To avoid this, our system has a signal ground, \perp , and a power ground, \perp , which are independently connected to one central point on the chassis. Signal ground is connected at only one point, and signal cable shields are connected to the signal ground. All other cable shields are connected to power ground^{41,42}.

SYMBOLS:

R	Resistor
C	Capacitor
D	Diode
Q	Transistor
P	Potentiometer, ganged or trim.
L	Pilot light
T	Transformer
S	Switch
F	Fuse
	Power ground
	Signal ground
	Socket pin connection
	Jumper
	Booster
	Operational amplifier
	Wheatstone bridge

ELECTRONIC CIRCUITS:

The six boards contain a regulated power supply, smoothed high current supply, oscillator and clamps, common mode rejection amplifier and current boosters, preamplifier and demodulator, and dc-ac switching circuit.

Trim potentiometers, P_1 and P_2 , for initial adjustments are located on the regulated power supply board. All operating controls (potentiometers for vertical and horizontal symmetry, ganged potentiometers for frequency and amplitude adjustment of the square-wave, potentiometers for the fine and coarse adjustments of the thermal conductivity bridge, attenuator for the output signal, pilot lamps, and switches) are mounted on the front panel of the instrument. A fuse and shielded connectors for supply, input and recorder are mounted on the back of the panel. Transformers are mounted directly on the chassis. The circuits will be discussed in the order given above.

The Regulated Power Supply: Fig. 5

The regulated power supply is electrically symmetrical with respect to ground. The top half will be discussed first and then the variations in the bottom half will be explained.

A rectifier, D_1 , and storage capacitor, C_1 , form the heart of the power supply. Resistor R_3 provides a short circuit protection for the transistor pair Q_1 and Q_2 . Capacitor C_2 along with resistors R_1 and R_2 act as a filter for the base current of transistor Q_2 ⁴³. The transistor reference amplifier RAI amplifies the error signal developed between the reference voltage at the emitter of this transistor and a fraction of the positive output determined by potentiometer P_1 . The amplified error signal forms the input to pass transistor Q_2 via Darlington transistor Q_1 which decreases output impedance⁴⁴. Capacitor C_3 improves high frequency stability. To allow remote sensing of the output voltage, the top lead of R_4 is brought out to a connector pin. Diode D_2 serves to prevent the output from going high in the event of an open circuit in the sensing lead.

The bottom half is based on a similar circuit, but to insure symmetry, the positive regulated output serves as a reference voltage for the negative supply. A transistor pair, Q_3 and Q_4 , rather than single transistor with grounded emitter, is used as comparison amplifier, to improve thermal tracking of the 2 outputs.

Remote sensing eliminates stray output impedance due to connector resistance. Two separate contacts at pin connections, 3 and 13, are provided for current paths for ac return and dc ground to prevent ac pick-up.

The values of the components are chosen to provide +15 and -15 volts regulated at approximately 100 mA. The voltages are adjusted to the

nearest 0.01 volt with the two trim potentiometers, P_1 and P_2 .

BOARD I

REGULATED POWER SUPPLY

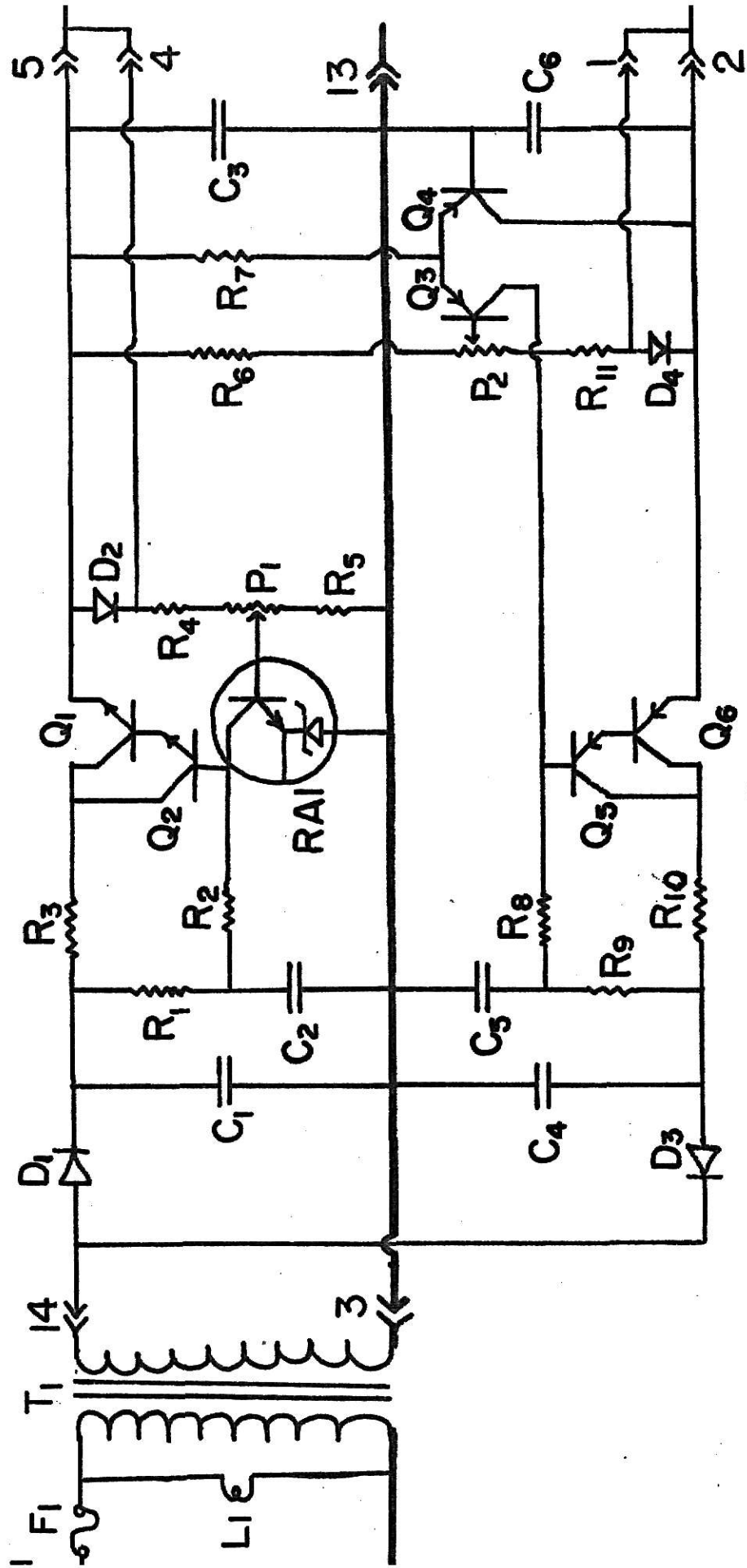


Fig. 5

The Smoothed High Current Supply: Fig. 6

The circuit produces +14 and -14 volts filtered at up to 400 mA. The bases of the transistors, Q₇ and Q₈, are powered by +15 and -15 volts respectively. The resistors act as protective elements for the transistors.

BOARD II

SMOOTHED HIGH CURRENT SUPPLY

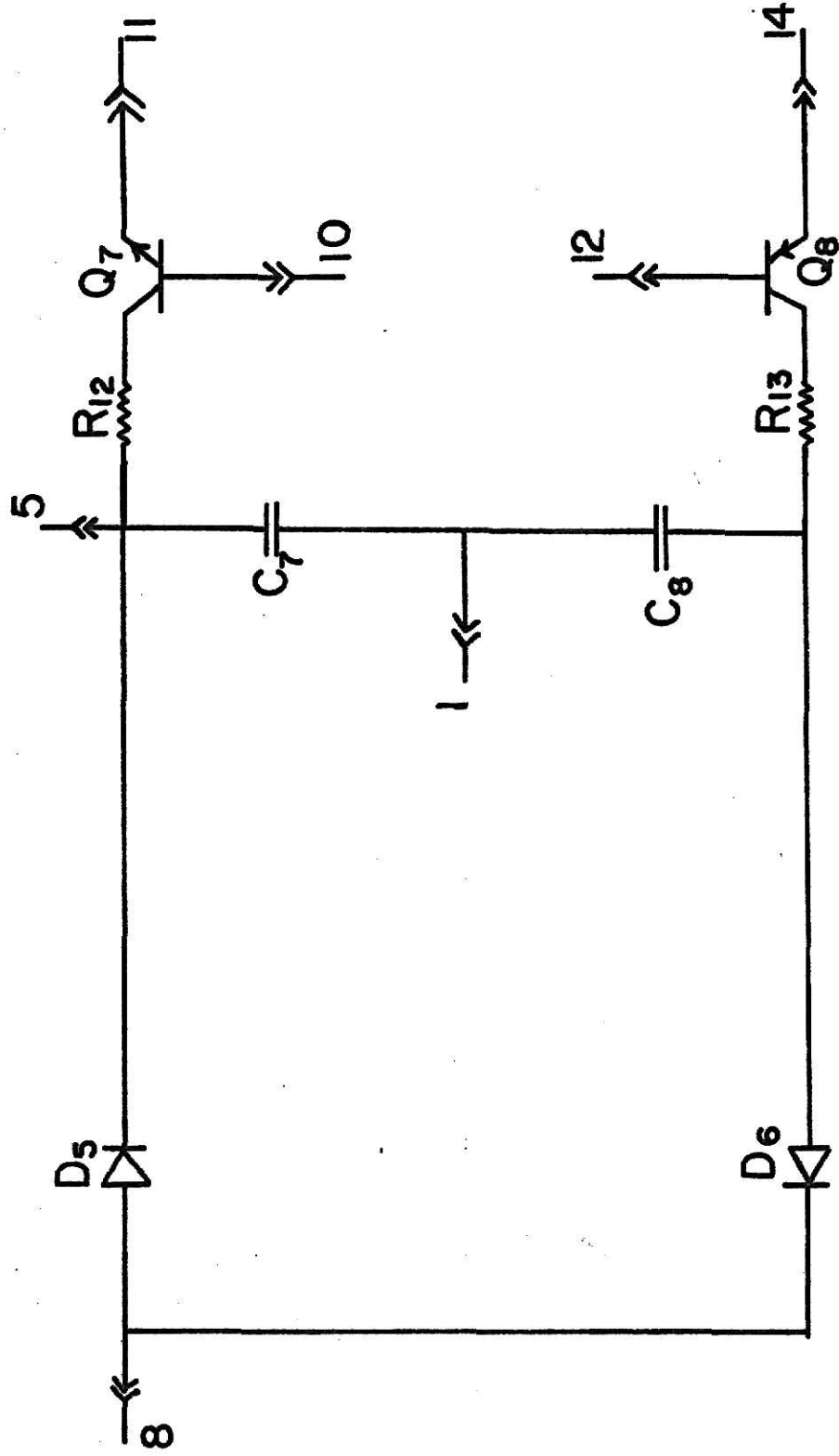


Fig.6